

Physico-Chemical Features and Subsurface Nature of Coastal Dunes on Bozcaada Island, NW Turkey

Mustafa Avcioğlu¹, Ahmet Evren Erginal^{2,*}, Muhammed Zeynel Öztürk³, Alper Demirci⁴, Yunus Levent Ekinci⁵, Murat Türkeş⁶, Ersin Karabacak⁷, Ali Sungur⁸, Hasan Özcan⁸, Rezzan Ekinci⁹, Gülsen Erginal¹⁰

¹Çanakkale Onsekiz Mart University, Department of Geological Engineering, 17020, ÇANAKKALE-TR

²Ardahan University, Department of Geography, 75000, ARDAHAN-TR

³Niğde University, Department of Geography, 51240, NİĞDE-TR

⁴Bitlis Eren University, Department of Geophysical Engineering, 13000, BITLIS-TR

⁵Bitlis Eren University, Department of Archaeology, 13000, BITLIS-TR

⁶Middle East Technical University, Affiliated Faculty at the Department of Statistics, 06800, ANKARA-TR

⁷Çanakkale Onsekiz Mart University, Department of Biology, 17020, ÇANAKKALE-TR

⁸Çanakkale Onsekiz Mart University, Department of Soil Sciences, 17020, ÇANAKKALE-TR

⁹Bitlis Eren University Campus, Lodging Buildings, R4 No: 20, 13000, BITLIS-TR

¹⁰Ardahan University, Vocational School of Çıldır, 75400, ARDAHAN-TR

Corresponding author. Tel: +90 534 9264784

E-mail: aerginal@gmail.com

Received 28 Nov 2014

Accepted 05 Jan 2015

Abstract

We studied the composition, vegetation cover, wind regime characteristics and subsurface nature of a coastal dune field on the west coast of Bozcaada Island, NW Turkey. Performing Electrical Resistivity Tomography (ERT) technique, we determined that dune sands with a thickness of ~11-13 m cover the underlying Miocene basement, as confirmed by an abrupt increase in resistivity as from lithological boundary. The results demonstrate that foredune terraces and ridges differ from swales from various points of view. The foredune sands are characterized by average contents of over 82% medium to fine-sized angular sands, especially quartz (85%), based on X-ray fluorescence spectroscopy (XRF) data, CaCO₃ (1.15%) and organic matter (0.19%). On the other hand, swales are composed on average of 59% medium to fine sands, a mixture of silt and clay (13%), very coarse sands and small-size gravels (28%). In addition to the different grain size distribution, swale sediments have conspicuously lesser amounts of SiO₂ (78%), higher amounts of CaCO₃ (5.6%) and organic matter (0.8%). Wind climatology analysis showed the predominance of a northerly (mainly NNE) near surface wind circulation over Bozcaada throughout the year with high wind speeds of maximum 7.4 m/s. Nevertheless, the existing sand transport and associated development of foredune forms and blowouts in the dune field relates considerably to the bimodal distribution of northerly winds (NNW and NNE). Although the coastal dune area is capped by a variety of dune plants, blowout development is highly active, in particular, on the northeast section of the dune field.

Keywords: Dune sand, electrical resistivity, wind climatology, Bozcaada Island, NW Turkey.

Introduction

Turkey has a long shoreline (8333 km including the Sea of Marmara and islands) because it is circumvented by the Black Sea (1701 km-long) to the north, the Aegean Sea (3484 km-long) to the west and the Mediterranean (1707 km-long) to the south (Sesli et al. 2009). A great quantity of sediment consisting of approximately 175 million t⁻¹ is discharged by sediment-laden rivers into these seas as well as lakes and water reservoirs (Öztürk, 1996). However, this value

may reach up to 450 million t⁻¹, which exceeds the average sediment transportation rate of 320 mt⁻¹ of the European continent (Hamidi and Kayaalp, 2008). Thus, sediment transport to Turkey's coasts favors the development of coastal sand dunes, particularly on prograding deltaic environments and sheltered bays (Özcan, et al. 2009a). Özhan, (2005) reported that the total length of coasts where coastal dunes occur is 845 km in 110 different locations in Turkey (Uslu, 1989). Albeit this wide distribution, our knowledge of the

physico-chemical characteristics, flora and wind regime of the dune fields is rather scanty (Serteser, 2004; Özcan, et al. 2009a, b; Erginal, et al, 2009).

In this study, we are concerned mainly with the characteristics of coastal dunes on the west coast of Bozcaada Island, NW Turkey (Fig. 1a). We identified the morphological, floristic and

physico-chemical characteristics of the coastal dunes on the basis of geomorphological observations, grain size measurements, X-ray fluorescence spectroscopy (XRF) and scanning electron microscopy/energy dispersive X-ray spectroscopy (SEM/EDX) data. Electrical resistivity tomography (ERT) was used to define subsurface geometry of coastal dunes and underlying Miocene basement

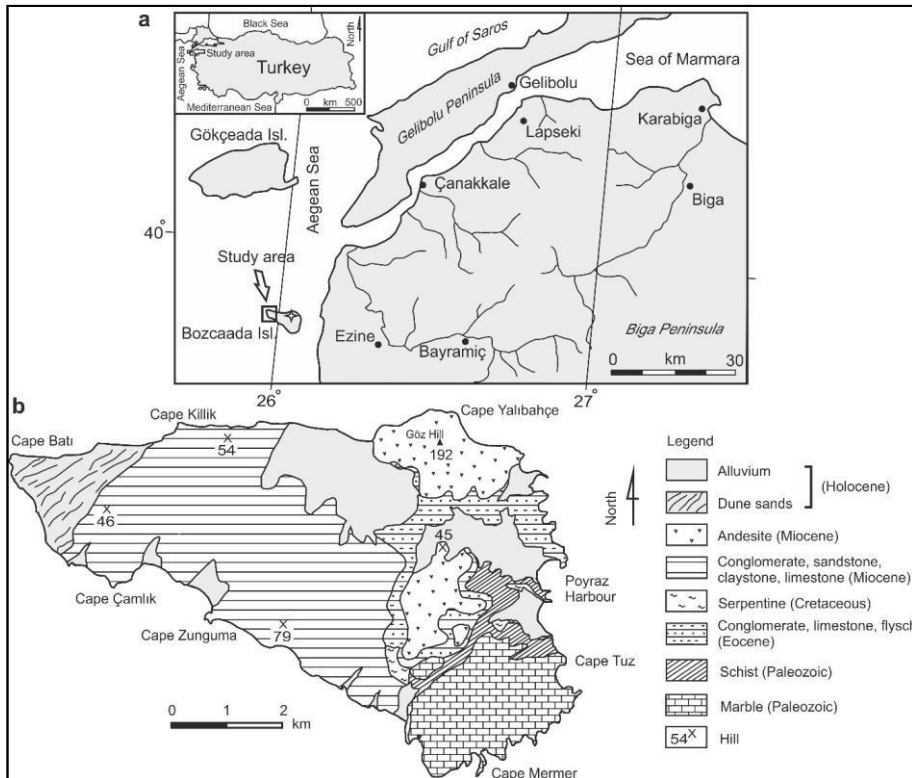


Figure 1. (a) Location map and (b) geology map of study area.

Physical Settings

Bozcaada Island, located 6 km west of the Biga Peninsula, NW Turkey, is a small island with an area of 36 km². The basement rocks on the island comprise marble and schist of Paleozoic age, which are overlain by Eocene basal conglomerate and flysch. Miocene is of widest extension, consisting of conglomerate, sandstone, claystone, limestone and andesite (Erguvanlı, 1955; Kalafatçıoğlu, 1963; Fig. 1b). The Holocene units are composed of alluvial deposits, beachrock, eolianite and coastal dunes (Kiyak and Erginal, 2009).

According to the rainfall regime classification of Turkey by Türkeş (1996, 1998), the study area has a Mediterranean-type rainfall regime. The period from April to October is mainly characterized by insufficient precipitation while the maximum precipitation shows up in the winter months. In terms of long-term averages, December is the wettest month (86 mm). The driest month, however, is August (about 5 mm). With respect to the monthly mean temperatures, the coldest and warmest months are February (8.3°C) and July (23.1°C), respectively. The island is of great significance for wind power production. In fact, the Bozcaada Wind Energy

Plant (BORES) forms the biggest available wind energy power plant in Turkey. It has reached an output of 131.35 MW (Şahin, 2008). Based on the Thornthwaite's Moisture Index (L_m) (1948), a dry sub-humid climate type is dominant at the Bozcaada station; a detailed climatic description is as follows: dry sub-humid, second mesothermal throughout the year, little or no water surplus during the year, with a summer concentration of thermal efficiency equal to a megathermal climate.

In the study area, the beach is sandy and is covered in many places by marine debris formed

generally by *Posidonia oceanica* (L.) Delile. The western promontory of the area is a rocky coast formed by low (1-2 m) sea cliffs and wave-cut platforms cut in Miocene limestone. The dune field, which encompasses an area of 2.25 km², constitutes 6% of the total surface area of the island. Coastal dunes lie between latitudes 39°50'48''-39°47'14'' north and longitudes 25°57'44''-26°04'59'' east. The dune field extends about 1.9 km on a southwest-northeast axis and has a rich plant community, consisting of 55 genus and 58 species belonging to 27 families (Karabacak et al. 2008).

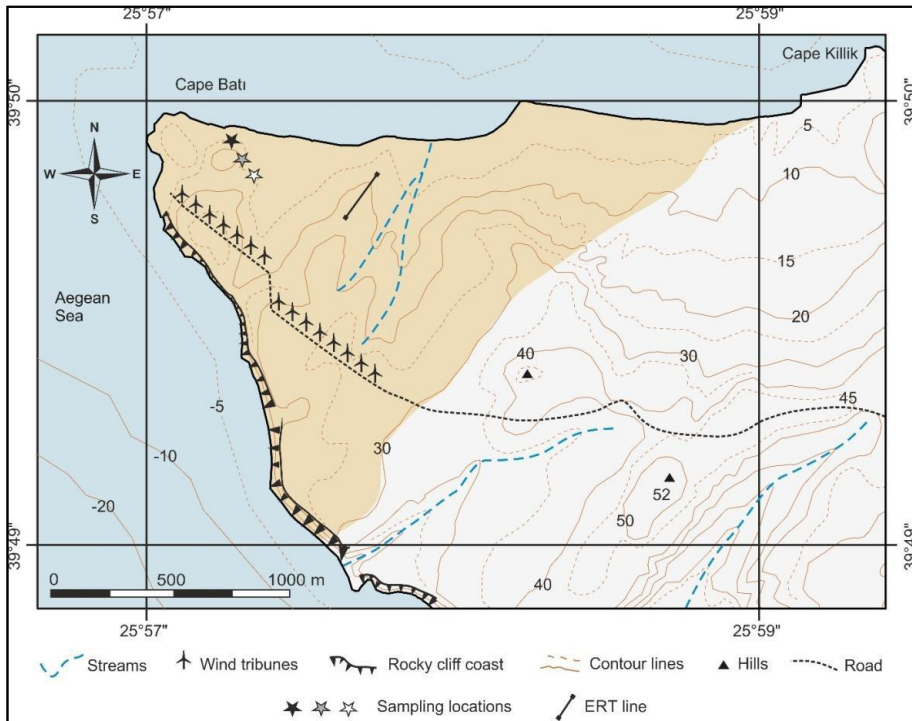


Figure 2. Map of sampling sites and ERT survey line. Black, gray and white stars show sampling pits from foredune terraces, ridges and swales, respectively.

Data and Methods

Sampling and Dune Sand Analyses

During field studies, different morphotypes of coastal dunes were recorded using GPS (Garmin ETREX). A total of 13 samples were taken from various depths of sampling pits dug along a representative line into incipient foredune terraces, ridges and swales (Fig. 2).

Sand samples were extracted from different horizons in consideration of their distinctive features (Soil Survey Staff 1993). From each sample of about 500 gr weight, CaCO₃ (%), electrical conductivity (EC), organic matter content and pH were measured. A Scheibler calcimeter (Schlichting and Blume, 1966) was used to determine total CaCO₃ contents. pH measurements were performed using a WTW

multi-parameter instrument (Grewelling and Peech, 1960). The content of organic matter within the samples was determined based on the Walkley-Black acid digestion method (Schlichting and Blume, 1966). A subsample weighing 200 g from each sample was also subjected to analysis by the hydrometry technique (Bouyoucos, 1951) in order to determine total clay, silt and sand contents.

To determine major oxides within samples, XRF analyses were carried out. The same samples were also analyzed by SEM (ZEISS EVO 50 EP) coupled with EDX (Bruker AXS XFlash) to understand the elemental composition and morphology (shape and size) of dune sands. These analyses were carried out in the Materials Research Centre of Izmir Institute of Technology. The Flora of Turkey (Davis, 1965-1985) was the main source used to identify plant specimens. Some doubtful identification was checked in Flora Europaea (Tutin et al. 1964-1980). Plants included in this list were deposited in the herbarium of the Biology Department of Çanakkale Onsekiz Mart University.

Wind and Water Budget Analyses

In the study, the monthly mean air temperature (°C) and monthly total precipitation (mm) series along with the long-term average wind speed (m/s) and monthly frequency of wind directions recorded at Bozcaada meteorology station of the Turkish State Meteorological Service (TSMS) were used. Long-term averages of wind speed and monthly frequency of wind directions were analyzed to determine the surface wind climatology. Thornthwaite's climate classification and water budget were calculated in consideration of the approach used in the WATBUG program (Willmott, 1977). For the water budget, we calculated the following parameters: unadjusted potential evapotranspiration (UPE) in mm; adjusted PE (APE) in mm; soil moisture storage (ST) in mm; actual evapotranspiration (AE) in mm; soil moisture deficit (DEF) and soil moisture surplus (SURP) in mm. Monthly PE values were calculated according to the Thornthwaite (1948) methodology. On the other hand, we calculated the Thornthwaite's Moisture Index using Thornthwaite's (1948) methodology as:

$$L_m = (100S - 60D)/PE$$

(1)

where, S is annual water surplus (mm) and D, annual water deficit (mm); PE is annual adjusted potential evapotranspiration (mm). Negative values of the moisture index are found in dry climates, while positive values are found in moist climates.

ERT Survey

ERT technique is an efficient geophysical tool to map the electrical resistivity characteristic of the subsurface. The technique offers fast and cost-effective high-resolution imaging of near surface resistivity pattern of shallow regions to depths of several tens of meters and provides useful information for characterizing disparate subsurface discontinuities, which can point to lithological variations (Erginal et al., 2013). Thus, in this study we used ERT technique to map both the thickness of the coastal dunes and its contact relation with the underlying bedrock. A line (Fig. 2) orientated nearly perpendicular to the coastline was assigned in the dune field considering one of the representative areas where coastal dunes have a thick accumulation of drifted sands. The apparent resistivities were gathered by means of GF ARES multi-electrode resistivity-meter system, with 41 electrodes spaced at 5.5 m intervals covering a total length of 220 m. Dipole-dipole electrode configuration was used for 10 data levels with dipoles of 5.5 and 11 m, and unit dipole separations of 1, 2, 3, 4, 5, 6, 2.5 and 3.5 m. The inversion of the measured apparent resistivity values was performed using the software package RES2DINV, which constructs a subsurface resistivity model based on iterative smoothness-constrained least squares (Loke and Barker, 1996). Due to the significance topographical relief along the survey line, the elevations of each electrode were measured by optical levelling and the topographical data were incorporated into inversion model for a more realistic interpretation.

Results and Discussions

The Nature of Incipient Foredues (Terraces and Ridges)

In the studied dune field, incipient foredues dominate the dune morphology. To define their nature, samples were collected from both terraces and ridges (Fig. 3a and b).

The measurement results obtained from a sea-facing slope of the dune terraces showed that sand is the predominant component (average 98%), characterized by angular quartz grains (Fig. 3c). More than 82% of dune materials belong to grain sizes ranging between 0.5 and 0.163, implying the predominance of medium to fine-grains. The clay and silt contents have proportions of 1.47% and 5.55%, respectively. Electrical conductivity values increase with depth. CaCO₃ and total organic matter contents are found in low amounts. XRF analyses also demonstrate that major oxides are found in descending order of confirming the prevalence SiO₂>Al₂O₃>K₂O>CaO>Na₂O>Fe₂O₃>TiO₂>MgO of quartz and plagioclase (Table 1) with no notable variation in the detected values. EDX results obtained from the same P1-1 and P1-4 also exhibit the existence of various elements in decreasing order of O>Si>C>Al>K>Fe>Mg>Ca (Table 1).

SiO₂ dominates with an average amount of 85%, confirming XRF results. None of the elements show a meaningful trend in depth in vertical section. The foredune terraces are covered with several salt-tolerant plant species shown in Table 2, consisting primarily of *Otanthus maritimus*.

Foredune ridges (P2 in Table 1) are, on the other hand, located behind the incipient dune terraces and are separated by transversal swales and blowouts (Fig.3d). They have elevations up to 10 meters and sharp crests owing to the development of through blowouts. Unlike dune terraces, ridges are not symmetrical in plan view. Their long axes are oblique to the present trend of the shoreline where they are interrupted by blowouts. Several types of dune plants well adapted to sea salt were observed on the ridges, dominated by *Ammophila arenaria* subsp. *Arundinacea*, *Eryngium maritimum*, and *Otanthus maritimus* (Table 2).

The measurements acquired from dune ridges showed an average of 93% for sand-sized grains. Similar to the foredune terrace sands, medium to fine-grains ranging in size between 0.5 mm and 0.163 mm are found in an average amount of 82%. The pH is slightly alkaline. EC values are significantly lower and major oxides are similar to those of the sands of foredune terraces. This is also the case for XRF data.

The Nature of Swale Materials

These interdune depressions have a large extension in the studied dune field and lie between northeast-southwest trending dune ridges. Swales actually follow morphologically former dry valleys, the edges of which were covered by dune ridges (Fig. 3e). On the northeast-inclined bottoms of these depressions, there is enrichment in vegetation cover listed in Table 2. Several physico-chemical characteristics and quantitative elemental analyses results from swale samples (P3 in Table 3) show that coarse and very coarse sands have an average amount of 28%. Medium and fine sands are, however, found in the proportion of about 59%. The rest (13%) of the composition is composed of a mixture of very fine sands and silty clay. All sand-size components have very poor roundness (Fig. 3f), similar to that of the foredune sands.

When compared with the foredune sands, this distribution indicates a conspicuous augmentation in the ratio of fine sediments (≤ 0.163 mm). The other differences are represented by an increase in the contents of total average organic matter and CaCO₃ as well as a decrease in the values of EC. In terms of the quantity of major oxides, XRF data display a similar distribution ratio to that of the foredune sands with the exception of an increase in CaO content. The EDX results from samples (Table 3) collected from the near surface (P3-1) and bottom (P3-3) of the sampling pit dug in the swale depression yielded more disparities, depicted by the elements aligned in descending order of O>Si>C>Al>Fe>Ca>K>Mg. All these data suggest that the chemical composition, grain size distributions, organic matter and CaCO₃ contents of swales differ from foredune materials.

Wind Regime, Moisture Conditions and Blowout Development

The wind characteristics of the island favor the development of various coastal dune forms in the study area. A Quickbird satellite image (Fig.4a) shows concordance of dune forms with the prevailing wind circulation. In particular, the distinct development of foredune ridges and blowouts is directly connected to the wind regime and surface moisture conditions during the dry season.

Wind turbines clearly indicate that, even though NNE is the prevailing wind of Bozcaada, northerly winds have a bimodal wind direction distribution, characterized by NNW and NNE (Fig.4b and c). The Bozcaada station shows strong long-term average annual mean wind speeds of about 7 m/s, exceeding this for both northerly (NNE) and southerly (S) surface wind circulations at ten meters over the study area (Table 4). Prevailing winds blow from NNE in all months except for June. In the months of May, June and July, the frequencies of north north-westerly and north north-easterly winds are nearly equal to each other. However, the prevailing wind direction is north north-west (NNW) only in June with a frequency of 21.87%, slightly more than that from NNE with a ratio of 21.47% (Fig.5).

During a long period of the year, particularly from November to April, southerly sector winds (mainly SSW, S, and SSE) also become somewhat effective in addition to the northerly sector winds. This is directly related to the increased number of mid-latitude and Mediterranean frontal cyclones in these months due to the significant seasonal migration of the polar front and associated upper-air polar jet to relatively low latitudes, leading to westerly and south-westerly air flows over the Mediterranean basin towards Turkey (Türkeş, 1998; Türkeş and Erlat, 2005; Türkeş et al. 2009).

Based on the assumption that the wind-blown removal of sand deflation is controlled by surface moisture conditions, a Thornthwaite water budget was prepared. The water budget shows that the island receives very low annual and monthly precipitation (Table 5).

The results obtained show a soil moisture surplus in winter months and a soil moisture deficit from May to October. The soil moisture deficit is particularly pronounced in July and August. The soil moisture surplus period is shortest through the months of January, February and March when the amount is lowest, with a total of 114 mm. The period of the soil moisture deficit (total of 443 mm) dominates over six months from May to October with severe summer dryness in July and August. November is a transition month when the water begins to accumulate in the soil, and the moisture increases due to the start of frontal precipitation events associated with both mid-latitude and Mediterranean cyclones over the region, respectively. Based on these results, the surface of the dune field is rather dry during the period between May and August.

The aforementioned wind characteristics and surface moisture conditions are of prime importance in deflation and erodibility of dune sands, thereby, in particular, allowing the development of blowouts and foredune ridges deprived of vegetation cover. In many places, several deflation basins occur on the crests of vegetation-deprived substrates of asymmetric ridges as result of the easy removal of dune sands.

These erosion hollows are blowouts *sensu strictu* and are either through or saucer-shaped, as being common elsewhere (Cooper, 1958; Bate and Ferguson, 1996; Hesp, 2002); the latter convert in several places into cup-or bowl-shaped depressions, encased in very coarse sands and very fine gravels, owing to the wind-induced deepening of shallow saucer blowouts (Hesp, 2002). The paragons of these circular or ellipsoidal-shaped depressions (diameter: 25x25 m and 25-60 m; depth: max: 10 m) are found in the southwest and west of the dune field and are located at the head of the through blowouts (Fig. 6a).

The deepening of these deflation basins is known to be associated with accelerated wind speed on or near the surface of the depression caused by the angle of incidence of effective winds (Hugenholtz and Wolfe, 2009), which is a well-known wind flow circulation pattern in coastal dune blowouts (Fraser et al. 1998;

Wang et al. 2007). Actually, with the lack of accurate near surface wind data, mean surface (10 meters) monthly wind speeds of Bozcaada show strong values (max: 7.4 m/s) (Table 4). Maximum wind speeds are mostly related with the N, NNE and NNW directions and partly with S and SSE directions both annually and in all months.

The through blowouts, however, are characterized by elongated depressions (Fig.6b), having steep and sharp lateral walls stabilized by dune plants. These dunes have long NE-trending axes that extend up to 600 m. Field observations showed that several blowouts seem to have ingenerated on the apex of foredune ridges and are weakly stabilized by plant canopies at both their margins. The removal of dune sands and subsequent initial opening of a blowout in these parts is likely associated with the accelerated speed of surface winds that act on the wide crests of foredunes (Smith1960). The bottom of the depressions, however, are stony and paleo soil-like; this coincides in many places with a surface of underlying fossiliferous Miocene limestones (Fig.6b), suggesting over-deepening through the stripping of loose blowout sands by northeast and southwest winds.

Subsurface Nature of Coastal Dunes

Figure 7 shows the model resistivity section with corrected topography, obtained after 5 iterations with an RMS error of 12 %. The SW-NE trending two-dimensional resistivity image displayed a depth range of ~17 m. The overall resistivity range in the image is ~15- to 2600 ohm-m. The resistivity tomogram obtained along a rugged and undulate topography crossing dune ridges, blowouts and parabolic dune depressions shows a clear contrast from the top down to the transition level cutting the underlying Miocene formations. The transition level lying at a depth between 13 m and 15 m is represented with a resistivity of ~150 ohm-m. From this level towards the deeper parts, resistivity values display an increasing trend, pointing to bedrock. The morphology carved in bedrock buried by dune sands is characterized by former valleys formed by NW flowing small streams on southwest-dipping Miocene strata. Throughout the contact level with the resistive basement, dune sands show a conformable

accumulation on the buried hummocky topography, which continues up to the surface of coastal dunes.

Nevertheless, coastal dunes display lower resistivity values less than 30 ohm-m with the exception of those determined in horizontal distance between 33 m and 132 m. This abnormal increase up to 2600 ohm-m was obtained along sharp dune crests due to the lack of lateral support that affects the resulting resistivity. This is confirmed by normal resistivity values between the distances of 148 m and 220 m of the survey line where coastal dunes have a uniform morphology sloping gently towards the sea. As result, ERT image demonstrated the depth of buried Miocene basement, the subsurface morphology of dune sands and the contact relationship between these two units.

Conclusions

We studied coastal sand dunes that rest on fossil-bearing Miocene limestones. Morphologically, various dune forms occur, such as saucer or ellipsoidal-shaped interdune depressions or blowouts, incipient foredune terraces and ridges and swales. ERT image obtained along a representative transect passing foredune ridges and blowouts displayed that dune sands have a thickness of about 11-13 m, which slightly increase seawards.

Towards the eastern most part of the dune field, relatively more fixed dunes exist. The dune field eventuates in a forest land comprising *Pinus brutia* developed on the basement rocks. The measured parameters of dune sands and effective wind climate yielded some consequential data on the nature and dynamics of the dune field. Foredune and swale sands were found dissimilar in recognition of both their content and grain sizes. Bidirectional (NW and SW) near surface wind circulation and long-term average high wind speeds account for the development of dune morphology. Notwithstanding the fact that the dune sands are capped by a number of plant species, effective wind activity does not render dune stabilization possible, except for swale depressions, which are covered with dense plant communities. Our study revealed that a combined interpretation of

the nature of dune sands, climatic data and dune sand development in coastal environments.

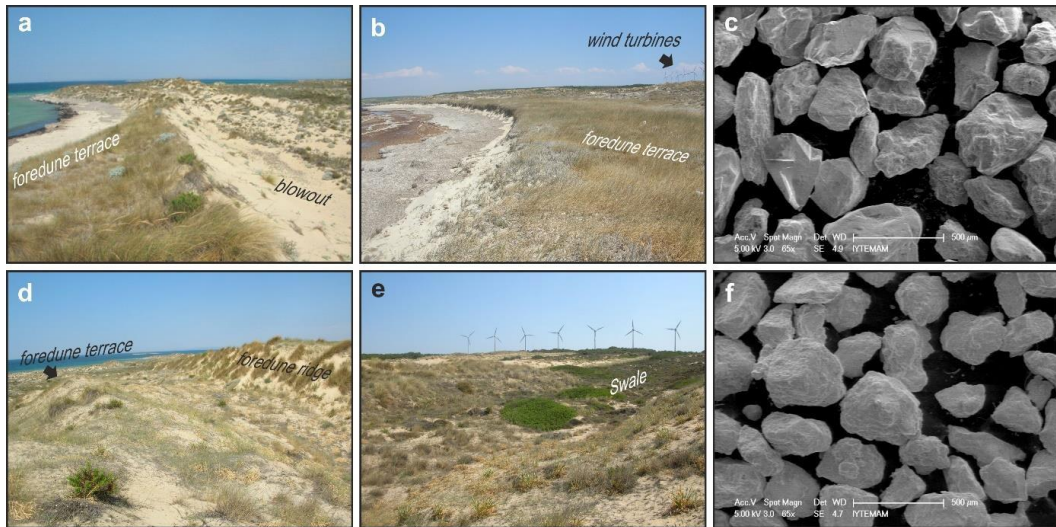


Figure 3. Field pictures and SEM images from the dune field. (a and b) Incipient foredune terraces along north beach. (c) SEM image of dune sands extracted from foredune terrace (sample P1-1 in Table 1). (d) Foredune ridges on northeast coast. (e) Swale near wind turbines on northwest coast. (f) SEM image of swale sands (sample P3-4 in Table 2).

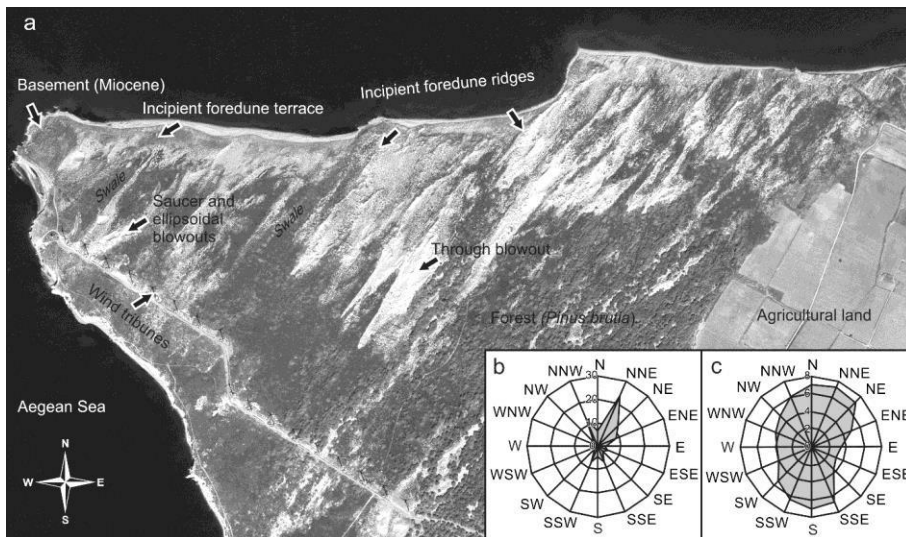


Figure 4. (a) Quickbird satellite image (2008) of dune field. (b) Long-term annual wind direction frequencies (as percentages), and (c) annual mean wind speeds (m s^{-1}) of Bozcaada meteorology station.

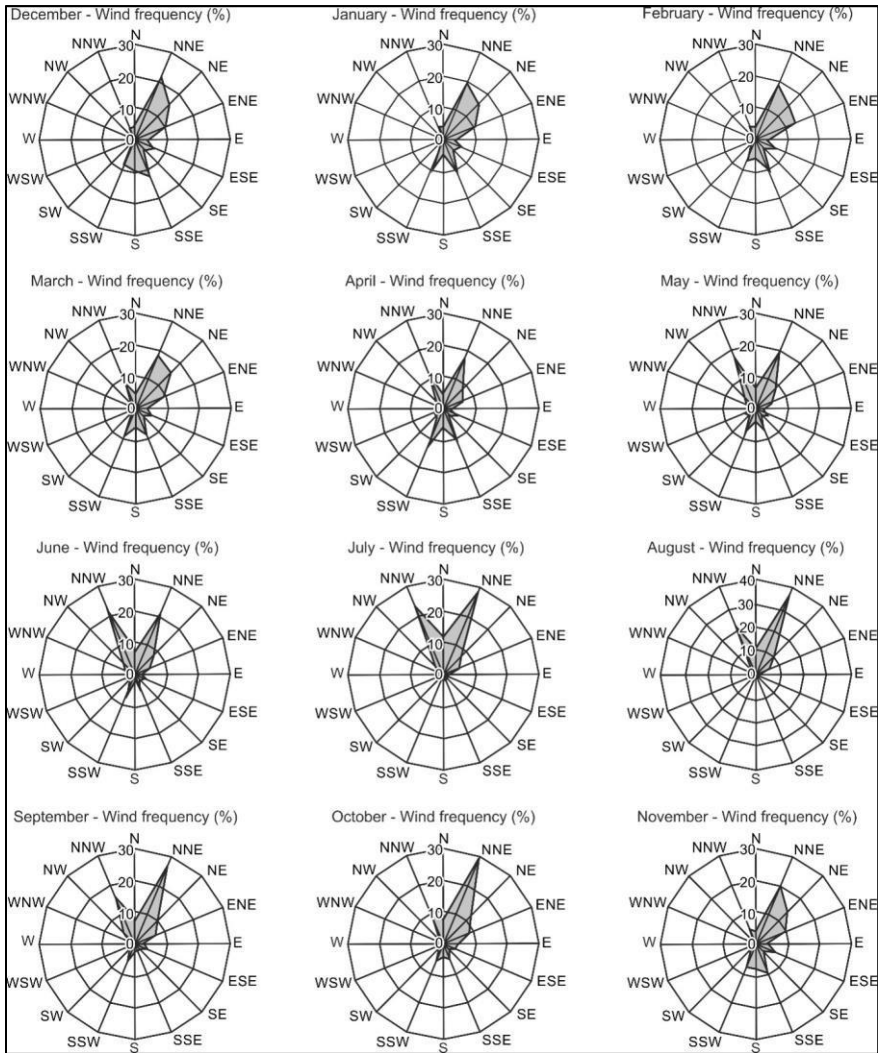


Figure 5. Monthly variations of wind direction frequencies (as percentages) of Bozcaada station.

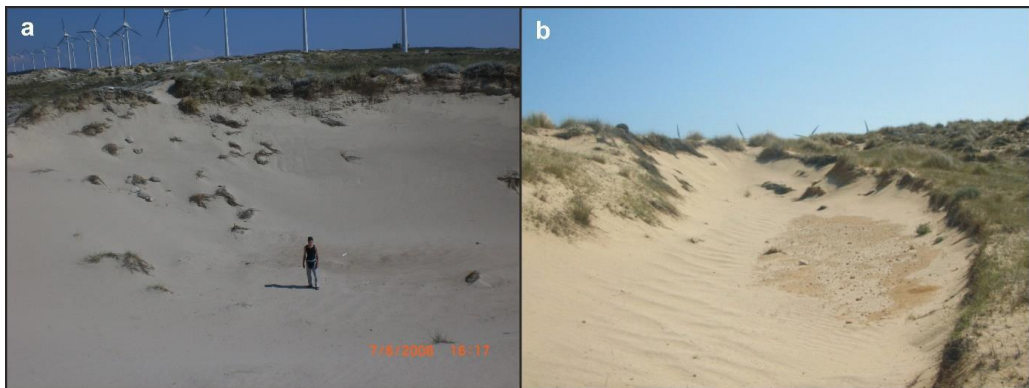


Figure 6. (a) Saucer-shaped blowout. Please see person's height for scale (1.80 m). (b) Shallow through blowout, bottom of which corresponds to emerged Miocene basement.

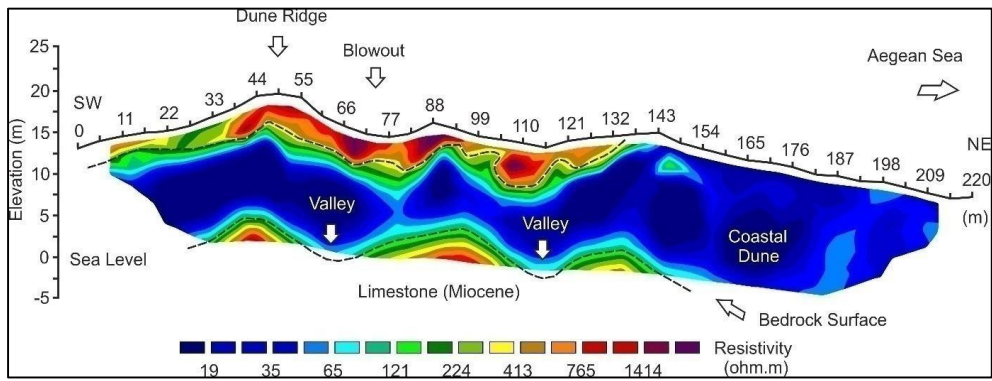


Figure 7. Electrical resistivity tomogram of surveyed line obtained from the inversion of apparent resistivity data.

Table 1 Several measured parameters of incipient foredune materials. P1 and P2 refer to samples taken from dune ramp slope and ridge, respectively.

Measured parameters					Grain size (mm)				
Profile	EC	pH	%CaCO ₃	%O.M.	2-1	1-0.5	0.5-0.25	0.25-0.163	≤0.163
p1-1	260	7.74	1.10	0.28	0.15	3.99	49.05	43.65	3.08
p1-2	635	8.25	1.88	0.32	0.45	11.66	61.6	25.12	1.09
p1-3	567	8.16	1.80	0.20	2.09	38.1	42.63	16.31	0.77
p1-4	616	7.95	1.88	0.28	0.34	8.4	56.36	33.45	1.43
p2-1	165.2	7.92	1.33	0.11	3.55	12.73	47.11	33.96	2.63
p2-2	144.3	7.98	1.25	0.14	1.27	11.73	50.57	33.98	2.45
p2-3	154.4	8.02	1.65	0.35	1.25	28.86	51.41	17.68	0.78
p2-4	207	8.13	1.41	0.07	0.89	9.87	52.51	34.05	2.61
XRF results									
Profile	SiO ₂	Al ₂ O ₃	TiO ₂	Fe ₂ O ₃	CaO	MgO	Na ₂ O	K ₂ O	
P1-1	85.41	7.96	0.03	0.48	1.26	0.01	1.49	1.85	
P1-2	84.79	8.02	0.09	0.41	1.57	0.01	1.32	1.92	
P1-3	84.94	6.97	0.06	0.45	2.41	0.11	0.80	1.80	
P1-4	85.09	8.22	0.09	0.38	1.36	0.01	1.34	1.99	
P2-1	85.22	7.60	0.11	0.44	1.73	0.01	1.27	1.91	
P2-2	85.12	7.83	0.12	0.45	1.48	0.01	1.48	2.00	
P2-3	85.68	7.61	0.08	0.38	1.52	0.01	1.08	1.93	
P2-4	84.68	8.20	0.16	0.48	1.50	0.01	1.51	1.89	
EDX results									
Profile	C	O	Mg	Al	Si	K	Ca	Fe	
P1-1	5.51	50.01	1.65	6.6	33.04	0.8	1.44	0.96	
P1-1	3.22	40.52	0.46	3.18	46.68	1.11	0.79	4.05	
P1-1	8.3	41.98	0.89	2.5	41.04	0.81	0.79	3.7	
P1-4	3.37	42.95	0.9	8.57	36.49	6.96	0.75	0	
P1-4	4.2	41.87	0.81	1.89	49.27	0.98	0.98	0	
P1-4	2.62	43.2	0.89	2.19	50.5	0.6	0	0	

Table 2. The lists of vegetation present in different zones in the Bozcaada dune field.

Taxon name	Life form	Location
Aetheorhiza bulbosa subsp. microcephala	Tuberous perennial	Foredune terraces, foredune ridges, interdune depressions
Ammophila arenaria subsp. arundinacea	Rhizomatous perennial	Foredune terraces, foredune ridges
Anthemis tomentosa subsp. tomentosa	Annual	Foredune terraces, foredune ridges
Centaurea spinosa var. spinosa	Perennial, cushion form	Foredune terraces, foredune ridges
Cynodon dactylon var. dactylon	Rhizomatous perennial	Foredune terraces, interdune depressions
Eryngium maritimum	Perennial herb	Foredune terraces, foredune ridges
Euphorbia paralias	Perennial herb	Foredune terraces, foredune ridges
Imperata cylindrica	Perennial herb	Foredune terraces
Medicago marina	Annual	Foredune terraces, foredune ridges
Otanthus maritimus	Perennial herb	Foredune terraces, foredune ridges, interdune depressions
Parapholis incurva	Annual	Foredune terraces
Elymus farctus subsp. farctus var. Farctus	Rhizomatous perennial	Foredune terraces
Cyperus capitatus	Rhizomatous perennial	Foredune ridges
Elymus elongatus subsp. elongatus	Rhizomatous perennial	Foredune ridges
Glaucium flavum	Biennial	Foredune ridges, interdune depressions
Pancratium maritimum	Bulbous perennial	Foredune ridges
Anthyllis hermanniae	Perennial shrub	Interdune depressions
Avena barbata	Annual	Interdune depressions
Blackstonia perfoliata	Annual	Interdune depressions
Bromus tectorum	Annual	Interdune depressions
Carlina corymbosa	Perennial herb	Interdune depressions
Cistus creticus	Perennial shrub	Interdune depressions
Coridothymus capitatus	Perennial shrub	Interdune depressions
Dactylis glomerata subsp. hispanica	Perennial herb	Interdune depressions
Dorychnium hirsutum	Perennial shrub	Interdune depressions
Echium angustifolium	Perennial herb	Interdune depressions
Erodium cicutarium subsp. cicutarium	Annual	Interdune depressions
Eryngium campestre var. campestre	Perennial herb	Interdune depressions
Fumana thymifolia var. thymifolia	Perennial shrub	Interdune depressions
Helichrysum stoechas subsp. barrelieri	Perennial	Interdune depressions
Hypochoeris glabra	Annual	Interdune depressions
Juncus acutus	Perennial	Interdune depressions
Lagurus ovatus	Annual	Interdune depressions

Limonium virgatum	Perennial herb	Interdune depressions
Malcolmia flexuosa	Annual	Interdune depressions
Medicago constricta	Annual	Interdune depressions
Onobrychis caput-galli	Annual	Interdune depressions
Orobanche ramosa	Annual parasites	Interdune depressions
Phragmites australis	Rhizomatous perennial	Interdune depressions
Pinus brutia	Tree	Interdune depressions
Pistacia lentiscus	Perennial	Interdune depressions
Rubia tenuifolia subsp. tenuifolia	Perennial sub-shrub	Interdune depressions
Sarcopoterium spinosum	Perennial, cushion form	Interdune depressions
Scipoides holoschoenus	Perennial herb	Interdune depressions
Shoenus nigricans	Perennial herb	Interdune depressions
Teucrium polium	Perennial herb	Interdune depressions
Thymelaea tartonraira	Perennial shrub	Interdune depressions
Tragopogon porrifolius	Annual	Interdune depressions
Vulpia membranacea	Annual	Interdune depressions
Osyris alba	Perennial, semiparasites	Interdune depressions

Table 3. Several measured parameters of swale materials.

Measured parameters					Grain size (mm)				
Profile	EC	pH	%CaCO ₃	%O.M.	2-1	1-0.5	0.5-0.25	0.25-0.163	≤0.163
P3-1	182.3	8.18	3.45	0.84	7.48	12.91	26.89	38.32	14.31
P3-2	213	8.07	3.29	0.57	5.94	13.46	27.35	38.69	14.53
P3-3	190.4	7.92	3.14	0.47	6.61	15.5	26.76	38.19	12.83
P3-4	247	8.07	12.54	1.33	22.16	28.35	21.77	17.38	10.32
XRF results									
Profile	SiO ₂	Al ₂ O ₃	TiO ₂	Fe ₂ O ₃	CaO	MgO	Na ₂ O	K ₂ O	
P3-1	82.28	7.87	0.15	0.69	2.84	0.01	1.25	1.92	
P3-2	81.47	7.93	0.15	0.75	3.34	0.01	1.13	1.90	
P3-3	81.65	7.78	0.13	0.66	3.41	0.01	1.15	1.85	
P3-4	66.93	8.11	0.24	1.73	10.01	0.54	0.73	1.74	
EDX results									
Profile	C	O	Mg	Al	Si	K	Ca	Fe	
P3-1	9.38	40.20	2.22	9.35	24.98	3.67	4.78	5.51	
P3-1	9.58	46.53	2.22	10.48	25.24	2.39	1.11	2.47	
P3-1	14.16	25.95	1.34	5.83	15.26	2.21	2.14	33.11	
P3-4	9.94	41.69	1.82	8.01	22.74	3.41	12.40	0	
P3-4	7.76	43.85	1.65	6.36	34.34	0.65	5.40	0	
P3-4	9.71	42.78	2.39	9.60	19.10	2.94	1.49	0	

Table 4 Long-term monthly and annual mean wind speeds ($m s^{-1}$) arranged in accordance with 16 (8 main and 8 interval) directions and long-term averages of monthly and annual mean wind speeds ($m s^{-1}$) of Bozcaada station regardless of direction. (*) Bold indicates the maximum mean and highest wind speeds that month.

Direction	Month												Annual
	J	F	M	A	M	J	J	A	S	O	N	D	
N	9.2(*)	7.6	8.6	6.0	6.0	5.7	7.1	6.8	7.1	7.7	6.8	9.2	7.1
NNE	8.7	9.1	8.2	6.6	6.0	5.5	6.5	7.1	7.1	8.4	8.2	8.5	7.4
NE	8.2	9.0	7.7	5.7	5.5	5.2	4.9	6.1	5.7	6.8	7.9	8.8	7.1
ENE	5.7	6.2	5.8	3.9	3.3	3.0	4.0	4.8	3.7	4.3	5.3	5.8	4.9
E	3.8	4.6	4.2	2.5	2.6	2.2	2.7	2.7	2.7	3.2	3.6	4.0	3.4
ESE	3.8	4.1	3.1	3.0	2.1	1.8	1.8	2.0	2.0	2.3	3.1	3.7	3.0
SE	5.3	5.0	4.1	3.2	2.4	2.4	1.4	1.8	2.1	2.7	3.8	4.8	3.6
SSE	7.8	8.4	7.3	6.4	5.2	3.7	3.0	2.6	4.5	5.7	6.7	8.1	6.7
S	7.7	8.2	7.8	6.5	5.7	4.7	2.6	3.8	5.0	6.1	7.4	7.9	7.0
SSW	8.5	7.7	7.1	6.2	5.0	4.7	3.6	4.4	4.6	5.5	6.7	8.2	6.4
SW	7.1	6.3	6.5	5.4	4.4	4.8	3.7	3.5	4.6	4.6	6.0	6.4	5.3
WSW	4.9	4.4	4.3	4.3	3.8	3.8	3.7	3.7	3.7	3.7	3.5	4.1	4.0
W	5.1	4.5	4.8	2.9	3.2	3.9	3.4	4.5	4.3	3.3	3.0	4.1	3.9
WNW	4.0	4.3	4.5	4.0	4.2	4.3	4.5	4.4	4.4	5.4	4.1	4.4	4.4
NW	2.8	3.6	4.4	4.3	4.9	5.4	5.6	6.0	5.6	4.8	3.7	4.6	5.0
NNW	5.9	5.6	6.4	5.5	5.3	5.8	6.6	7.0	6.7	6.1	5.2	5.7	6.2
Average	6.2	6.2	5.9	4.8	4.4	4.2	4.1	4.5	4.6	5.0	5.3	6.1	5.3

Table 5 Thornthwaite water budget of Bozcaada meteorology station for period 1975-2005.

Variables	Jan	Feb	Mar	Apr	May	June	July	Aug	Sep	Oct	Nov	Dec	Total
TEMP ¹	8.4	8.3	9.8	13.6	17.3	21.5	23.1	23.0	20.7	16.9	12.7	9.8	
UPE ²	22	21	28	47	68	96	108	107	91	66	42	28	
APE ³	18	18	28	51	84	119	136	126	93	63	35	23	794
PREP ⁴	70	57	52	40	25	11	6	5	17	25	70	86	465
DIFF ⁵	52	40	23	-11	-59	-108	130	-120	-76	-38	35	63	
ST ⁶	100	100	100	90	49	16	4	1	1	0	36	99	
CST ⁷	1	0	0	-10	-40	-33	-12	-3	-1	0	35	63	
AE ⁸	18	18	28	51	65	44	18	8	18	25	35	23	351
DEF ⁹	0	0	0	1	19	75	118	117	75	37	0	0	443
SURP ¹⁰	51	40	23	0	0	0	0	0	0	0	0	0	114

(1) Air temperature (TEMP) in °C, (2) Unadjusted potential evapotranspiration (UPE) in mm, (3) Adjusted potential evapotranspiration (APE) in mm, (4) Precipitation (PREC) in mm, (5) Precipitation minus APE (DIFF) in mm, (6) Soil moisture storage (ST) in mm, (7) Change in storage from the preceding month (CST) in mm, (8) Actual evapotranspiration (AE) in mm, (9) Soil moisture deficit (DEF) in mm, (10) Soil moisture surplus (SURP) in mm

Acknowledgement

We thank Dr. Aydın Büyüksaraç for his permission to use resistivity meter in the research. The modeling procedures of the resistivity data were carried out at the Earthquake Monitoring and Data Processing Laboratory (DEIVIL) in

Department of Geophysical Engineering at Çanakkale. Graham Lee is thanked for putting effort into linguistic corrections of the paper. This study was supported financially by the project no 2008/32 and partially supported by the project no 2010/162 of the Research Foundation of Çanakkale Onsekiz Mart University.

References

- Bate, G., Ferguson, M. (1996). Blowouts in coastal foredunes. *Landscape and Urban Planning*, 34 (3-4), 215-224.
- Bouyoucos, G.J. (1951). A recalibration of the hydrometer method for making mechanical analysis of soils. *Agronomy Journal* 43, 434-438.
- Cooper, W.S. (1958). Coastal sand dunes of Oregon and Washington. *Geological Society of America Memoir* 72. Waverly Press, Inc. Baltimore, MD.
- Davis, P.H. (1965-1985). Flora of Turkey and the East Aegean Islands, Volumes 1-9. Edinburgh: Edinburgh University Press.
- Erginal, A.E., Ekinçi, Y.L., Demirci, A., Avcıoğlu, M., Öztürk, M.Z., Türkes, M., Yiğitbaş, E. (2013). Depositional characteristics of carbonate-cemented fossil eolian sand dunes: Bozcaada Island, Turkey. *Journal of Coastal Research* 29 (1), 78-85.
- Erginal, A.E., Kiyak, N.G., Özcan, H. (2009). Optically Stimulated Luminescence to date coastal dunes and a possible Tsunami layer on the Kavak delta (Saros Gulf, NW Turkey). *Turkish Journal of Earth Sciences* 18 (3), 465-474.
- Erguvanlı, K. (1955). Geological study of the Bozcaada Island. *Bulletin de la Société Géologique de France* 6, 399-401 (in French).
- Fraser, G.S., Bennett, S.W., Olyphant, G.A., Bauch, N.J., Ferguson, V., Gellasch, C.A., Millard, C.L., Mueller, B., O'malley, P.J., Way, N., Woodfield, M.C. (1998). Windflow circulation patterns in a coastal dune blowout, south coast of Lake Michigan. *Journal of Coastal Research* 14 (2), 451-460.
- Grewelling, T., Peech, M. (1960). Chemical Soil Test. Cornell University *Agricultural Experiment Station Bulletin*, New York.
- Hamidi, N., Kayaalp, N. (2008). Estimation of the amount of suspended sediment in the Tigris River using artificial neural networks. *Clean-Air Soil Water*, 36 (4), 380-386.
- Hesp, P. (2002). Foredunes and blowouts: initiation, geomorphology and dynamics. *Geomorphology*, 48 (1-3), 245-268.
- Hugenholtz, C.H., Wolfe, S.A. (2009). Form-flow interactions of an eolian saucer blowout. *Earth Surface Processes and Landforms*, 34 (7), 919-928.
- Kalafatçıoğlu, A. (1963). Geology of the environs of Ezine and Bozcaada; age of limestones and serpanites. *Bulletin of the Mineral Research and Exploration* 60, 60-69 (in Turkish).
- Karabacak, E., Erginal, A.E., Özmen, H. (2008). Flora and mapping of dune vegetation of the Bozcaada-Batıburnu area. Symposium of Bozcaada Values, Abstracts Book, Aynalı Pazar Yayınevi, Bozcaada, 183-191 (in Turkish).
- Kiyak, N.G., Erginal, A.E. (2009). Optical Stimulated Luminescence dating study of eolianite on the Island of Bozcaada, Turkey: preliminary results. *Journal of Coastal Research*, 26 (4), 673-680.
- Loke, M.H., Barker, R.D. (1996). Rapid least-squares inversion of apparent resistivity pseudosections using a quasi-Newton method. *Geophysical Prospecting* 44 (1), 131-152.
- Özcan, H., Akbulak, C., Kelkit, A., Tosunoğlu, M., Uysal, I. (2009a). Ecotourism potential and management of Kavak Delta. *Journal of Coastal Research* 25 (3), 781-787.
- Özcan, H., Erginal, A.E., Akbulak, C., Sungur, A., Bozcu, M. (2009b). Physico-chemical characteristics of coastal dunes on the Saros Gulf, Turkey. *Journal of Coastal Research* 26 (1), 132-142.
- Özhan, E. (2005). Coastal area management in Turkey. Priority Actions Programme Regional Activity Centre (PAP/RAC). Coastal Area Management in Turkey, Split..
- Öztürk, F. (1996). Suspended sediment yields of rivers in Turkey. In: *Erosion and Sediment Yield: Global and Regional Perspectives*. Proceedings of the Exeter Symposium: 65-71.
- Şahin, A.D. (2008). A Review of Research and Development of Wind Energy in Turkey. *Clean-Soil Air Water* 36 (9), 734-742.
- Schlichting, E., Blume, E. (1966). *Bodenkundliches practicum*. Hamburg und Berlin: Verlag Paul Parey.

- Soil Survey Staff, (1993). Soil Conservation Service National Soil Survey Handbook Part 618, Title 430-VI, US Dept of Ag. (USDA), US Govt Printing Office, Washington DC.
- Serteser, A. (2004). Assessment of coastal dunes in Ceyhan Delta (Adana) with regards to vegetation and soil relationships. V. National Conference on Turkey's Coastal and Marine Areas, Abstracts Book, 1, 17-24 (in Turkish).
- Sesli, F.A., Karşlı, F., Çölkesen, I., Akyol, N. (2009). Monitoring the changing position of coastlines using aerial and satellite image data: an example from the eastern coast of Trabzon, Turkey. *Environmental Monitoring and Assessment* 153, 391-403.
- Smith, H.T.U. (1960). Physiography and photo interpretation of coastal sand dunes. Final Report Contract NONR - 2242(00), Office of Naval Research, Geographical Branch.
- Thorntwaite, C.W. (1948). An Approach toward a rational classification of climate. *Geography Review*, 38, 55-94.
- Tutin, T.G., Heywood, V.H., Burges, N.A., Moore, D.M., Valentine, D.H. (1964-1980). *Flora Europaea* Volume 1-5. Cambridge: Cambridge University Press.
- Türkeş, M. (1996). Spatial and temporal analysis of annual rainfall variations in Turkey. *International Journal of Climatology*, 16 (9), 1057-1076.
- Türkeş, M. (1998). Influence of geopotential heights, cyclone frequency and Southern Oscillation on rainfall variations in Turkey. *International Journal of Climatology*, 18 (6), 649-680.
- Türkeş, M., Erat, E. (2005). Climatological responses of winter precipitation in Turkey to variability of the North Atlantic Oscillation during the period 1930-2001. *Theoretical and Applied Climatology* 81 (1-2), 45-69.
- Türkeş, M., Koç, T., Sarış, F. (2009). Spatiotemporal variability of precipitation total series over Turkey. *International Journal of Climatology* 29 (8), 1056-1074.
- Uslu, T. (1989). Geographical Information on Turkish Coastal Dunes. European Union for Dune Conservation and Coastal Management Publications, Leiden.
- Wang, S., Hasi, E., Zhang, J., Zhang, P. (2007). Geomorphological significance of air flow over saucer blowout of the Hulun Buir sandy grassland. *Journal of Desert Research* 2007 (5), 745-749.
- Willmott, C.J. (1977). *Watbug: A Fortran IV Algorithm for Calculating the Climatic Water Budget*. Newark, Delaware: Water Resources Center, University of Delaware.
- Yu, Jian Zhen, Xiao-Feng Huang, Jinhui Xu, and Min Hu. (2005) "When aerosol sulfate goes up, so does oxalate: Implication for the formation mechanisms of oxalate." *Environmental science & technology* 39 (1), 128-133.
- Zuo, Yuegang, and Juerg Hoigne. (1992) "Formation of hydrogen peroxide and depletion of oxalic acid in atmospheric water by photolysis of iron (III)-oxalato complexes." *Environmental Science & Technology* 26, no. 5: 1014-1022.